CODE 132

VEGETATION DETECTION ON HERITAGE FAÇADES: LIMITATIONS OF NDVI AND A CASE-OPTIMIZED ALTERNATIVE

Soubrier, Philippe1-2; Vlaminck, Michiel2;
Luong, Hiep2;Van Den Bossche, Nathan1

1: Building Physics Research Group
Ghent University

2: IPI-URC-imec
Ghent University
e-mail: Philippe.Soubrier@ugent.be, web: https://ipi.ugent.be

ABSTRACT

Remote sensing technologies have emerged as essential tools for assessing the condition of heritage buildings, with applications ranging from documentation to conservation planning. This study specifically investigates the utility of the Normalized Difference Vegetation Index (NDVI) for detecting vegetation on façades of cultural heritage buildings. Employing hyperspectral imaging data acquired via an Unmanned Aerial Vehicle (UAV), this research evaluates NDVI's performance in the context of the Castle of Horst, a historical monument in Belgium undergoing restoration. The methodology includes photogrammetric reconstruction, radiance-to-reflectance correction using spectral reference panels, and systematic analysis of spectral data to distinguish vegetation from non-vegetated materials. The evaluation demonstrates NDVI's capability to detect vegetation accurately, while also revealing significant limitations such as sensitivity to varying illumination conditions and misclassification due to indirect lighting effects. To address these limitations, this paper proposes and validates a novel Case Optimized Index (COI), derived through exhaustive spectral band analysis, exhibiting superior classification accuracy compared to NDVI alone. Additionally, an XGBoost classifier further confirms the effectiveness of combining hyperspectral and RGB data, emphasizing the potential of machine learning techniques in enhancing vegetation detection accuracy. This research contributes practical insights into optimizing vegetation indices specifically for cultural heritage conservation, informing future methodologies for non-invasive façade assessment.

KEYWORDS: Remote Sensing; Hyperspectral Imaging; Cultural Heritage Conservation; Vegetation Detection; NDVI

1. INTRODUCTION

Remote sensing technologies offer substantial advantages in the assessment of building conditions, particularly in the context of cultural heritage conservation. Techniques such as RGB imaging effectively document the visual state of structures digitally. Coupled with photogrammetry and Unmanned Aerial Vehicle (UAV) flexibility, RGB imaging enables efficient and comprehensive documentation. Nevertheless, analysis confined to the visible spectrum alone is insufficient, as additional valuable information resides in other spectral regions.

Near-infrared (NIR) imagery has demonstrated significant potential within remote sensing, particularly regarding vegetation detection. Its applications extend across environmental monitoring, agriculture, and forestry [1]. The Normalized Difference Vegetation Index (NDVI) is among the most prominent indices used for vegetation detection, with successful implementation across numerous disciplines [2]. However, NDVI's application to the domain of cultural heritage buildings remains relatively unexplored.

This paper investigates the potential of NDVI specifically within the context of cultural heritage conservation. It builds upon previous research conducted by our research group, which examined hyperspectral imaging (HSI) methodologies in similar scenarios. Utilizing the Castle of Horst, a historical monument in Belgium, as a case study, this paper evaluates NDVI's effectiveness for vegetation detection on heritage façades. Furthermore, it addresses associated challenges, limitations, and potential future improvements and research directions.

1.1. NDVI Index: Historical Context and Original Development

Originally developed in 1969 [3], the NDVI was specifically designed to assess vegetation health and density. The index leverages differences in reflectance between the near-infrared (NIR) and red spectral bands, sensitive to leaf structure and chlorophyll absorption. In 1974, the NDVI formula was further refined for application on the Earth Resources Technology Satellite (ERTS-1) [4], later renamed Landsat-1, and is mathematically defined as follows:

$$NDVI = \frac{NIR - RED}{NIR + RED} \tag{1}$$

In formula (1), NIR and RED represent reflectance values corresponding precisely to Landsat-1's Multispectral Scanner (MSS) bands: band 7 for near-infrared (800–1100 nm) and band 5 for visible red (600–700 nm). NDVI values typically range from -1 to +1, higher positive values indicate denser, healthier vegetation, while negative or near-zero values correspond to sparse vegetation, bare soil, or non-vegetated surfaces.

1.2. NDVI Applications on Cultural Heritage Facades

Research on NDVI's specific application for cultural heritage buildings is limited. Previous studies have incorporated NDVI as an additional feature within classifiers designed to detect façade pathologies [5]. However, in certain cases, including NDVI did not significantly enhance the classification results compared to using only RGB and NIR data [6].

Outside the architectural context, more recent research has investigated similar vegetation types commonly found on façades, such as moss, algae, and lichen. One such investigation [7] explored the detection and health assessment of moss and lichen using UAV-mounted multispectral (MicaSense Altum with blue, green, red, red-edge, and near-infrared bands) and hyperspectral cameras (Headwall Hyperspec Nano, 240 bands, 400–1000 nm). The study tested both existing and newly developed NDVI variations, achieving high accuracy while also highlighting certain limitations.

In cultural heritage applications, vegetation detection primarily serves as an indirect indicator of moisture presence. Unlike efforts focusing specifically on immediate water detection [6-8], this paper emphasizes detecting vegetation as a longer-term indicator of moisture presence on façades.

1.3. Spectral Bands Analysis

The calculation of NDVI typically involves red and NIR bands, however, the specific wavelengths used can vary significantly depending on sensor characteristics and application requirements. Table 1 summarizes the spectral bands employed in previously mentioned studies. The variability depicted in Table 1, emphasizes the necessity of careful consideration when selecting bands and highlights the potential for further improvements tailored to specific use cases.

Table 1: Comparison NDVI band selection from various studies.

Study	Sensor	Red Band (nm)	NIR Band (nm)
Rouse et al. [4]	ERTS-1's MS camera	600-700	800-1100
Hemmleb et al. [5]	Multi-spectral laser scanner	670	980
Valença et al. [6]	Modified RGB DSLR	DSLR red	950-1200
Sandino et al. [7]	MicaSense Altum	661-675	814-870

Studies such as Sandino et al. [7] have successfully introduced subtle modifications to the NDVI formula through detailed analyses of hyperspectral data combined with multispectral imaging. They identified new bands exhibiting noticeable spectral peaks and valleys, including wavelengths at 480, 560, 655, 678, 740, 888, and 920 nm, specifically optimized for classifying different types of moss and lichen at various health stages and differentiating them from non-vegetated surfaces.

2. CASE STUDY: Castle of Horst

This paper extends previous research conducted by our research group [11], which utilized the Castle of Horst as a to restoration works due to its deteriorating condition. Its complexity in terms of diverse building materials, various historical restorations, and numerous pathologies renders it particularly suitable for hyperspectral imaging studies.

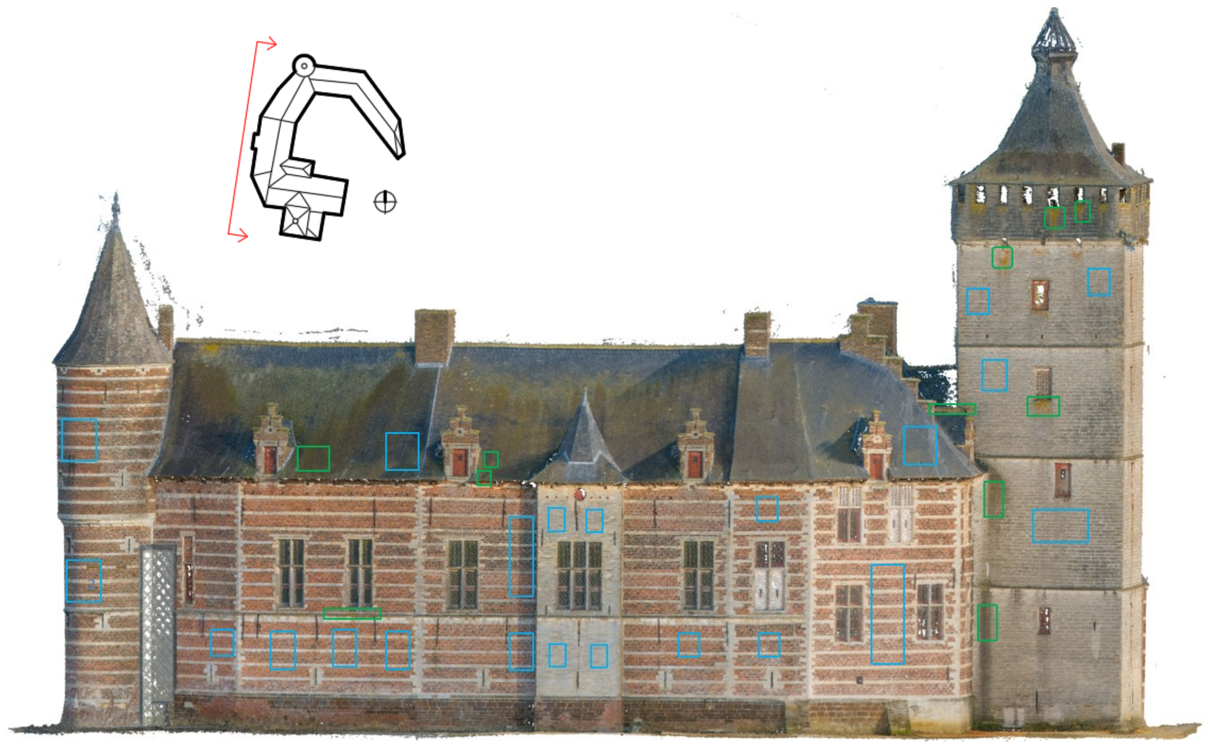

Figure 1: RGB - Western façade of the Castle of Horst.
Green sampling areas indicate vegetation, blue indicate non-vegetated materials.

2.1. Acquisition Methodology

The dataset is composed of a combined HSI and RGB point cloud, acquired using an UAV-based system. Specifically, a DJI Matrice 600 Pro drone equipped with imec's VIS-NIR hyperspectral payload was employed. This payload incorporates two distinct cameras, one covering the visible spectrum (VIS) and another for the near-infrared spectrum (NIR). The detailed specifications of this hyperspectral payload are presented in Table 2.

Table 2: Specifications HSI payload.

Parameter	Value
Spectral resolution (VIS)	16 bands ($\Delta\lambda \approx 9$ nm)
Spectral resolution (NIR)	15 bands ($\Delta\lambda \approx 17$ nm)
Spectral range	460 nm - 900 nm
FWHM	10 – 15 nm

Additionally, high-resolution RGB images were captured using a DJI Mini 4 drone. These images were integrated with the hyperspectral data through photogrammetry, resulting in a unified 3D reconstruction. The compactness and maneuverability of the DJI Mini 4 facilitated comprehensive image capture from multiple viewpoints, minimizing distortion and ensuring full coverage of the structure. Consequently, this dataset encompasses not only the external facades recorded by the hyperspectral payload but also includes challenging areas such as the inner court, lower sections, and rooftops.

2.2. Radiance to Reflectance Correction

Reflectance values are crucial for accurately calculating normalized difference indices, as these indices rely on consistent spectral measurements across different wavelengths. Variations in incoming illumination, caused by factors such as weather conditions or localized environmental interactions, significantly impact measured radiance values.

To correct for illumination variability due to weather conditions, a spectralon reference panel was utilized. This involved positioning reference panels with known reflectance characteristics at multiple locations on the facade and capturing it at different times throughout the acquisition process. Subsequently, during post-processing, these known reference values are used for the conversion of radiance measurements to standardized reflectance values ranging between 0 and 1. This widely adopted method effectively mitigates the influence of transient illumination variations on the dataset.

In contrast, correcting illumination discrepancies caused by environmental interactions presents a greater challenge due to their highly localized effects. Consequently, this paper's analysis will focus primarily on reflectance data acquired from the castle's western facade, which was directly exposed to sunlight during acquisition and lacked nearby vegetation that could alter incoming illumination.

3. EVALUATION

The hyperspectral point cloud is analyzed using the open-source software CloudCompare. Notably, normalized difference indices can also be integrated directly into the photogrammetry software, Metashape in this case study. Figure 2 illustrates the computed NDVI on each point, utilizing spectral bands at 802 nm (NIR) and 685 nm (RED).

The NDVI correctly identifies moss on window sills and horizontal facade elements (regions of interest (ROI) 1 and 5). The absence of a gutter adjacent to the southern tower is effectively indicated by a moss trace successfully detected on the tower's side (ROI 4). Conversely, the tower's upper region (ROI 6) is generally oversaturated, although healthy moss is indeed present but only beneath the openings. On the southern roof area (ROI 3), a gradient approximately matching reality from left to right is observed, however, vegetation health is overestimated. The northern roof region (ROI 2) erroneously indicates abundant healthy moss on the left side of the dormer, where moss is nearly absent in reality.

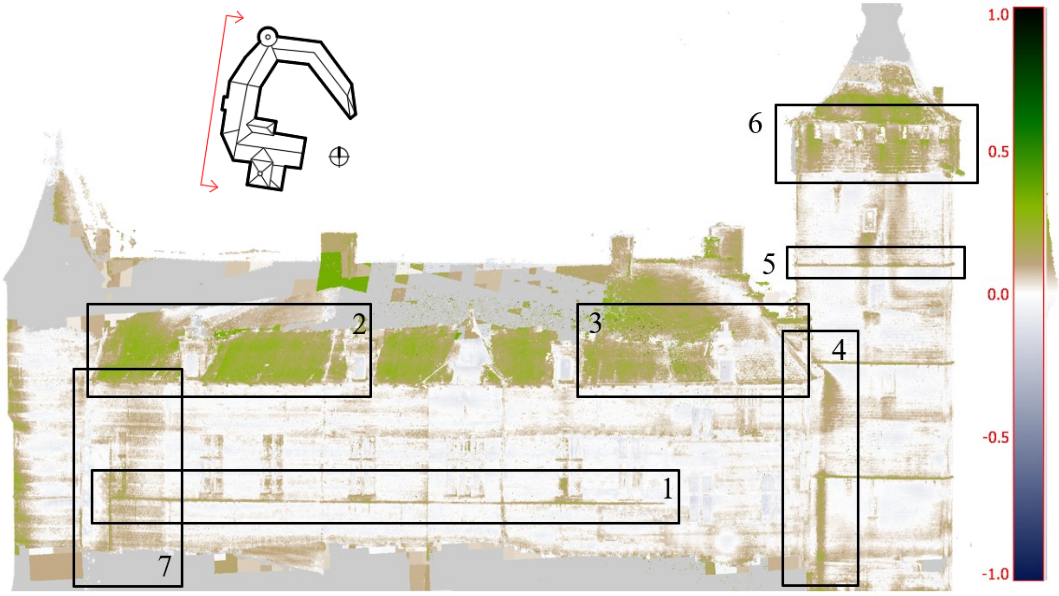

Figure 2: NDVI - Western façade of the Castle of Horst.

Despite uniform lighting during data acquisition, sections of the façade angled differently (ROI 7) reflect less direct light, increasing their susceptibility to indirect lighting. This phenomenon leads to bricks being mistakenly classified as vegetation. Such misclassification is even more prominent when using the Healthy–Stressed Moss Index (HSMI) [7], presented in Figure 3. HSMI is a normalized difference index defined as:

$$HSMI = \frac{740nm - 655nm}{740nm + 655nm} \tag{2}$$

Figure 3 underscores the suitability of HSMI for health assessment rather than detection, as it extensively overestimates vegetation presence, yielding numerous false positives. ROIs 1 and 2 reveal the index's sensitivity to varying illumination conditions and reinforce its role as a health indicator rather than a detection index, similar to many indices in this category.

Figure 3: Healthy–Stressed Moss Index (HSMI) - Western façade of the Castle of Horst.

4. OPTIMISATION

To optimize a normalized difference index specifically for vegetation detection in this case study, a brute-force method systematically tests combinations of the 31 hyperspectral bands alongside the 3 RGB bands. A binary annotation of the façade (as shown in Figure 1), representing the majority of façade materials at different orientations, serves as a reference. For each potential index, mean square errors between predicted and annotated vegetation states are calculated, where predictions range from -1 for non-vegetation to 1 for vegetation. The optimal combination identified through this exhaustive search produces the Case Optimized Index (COI):

$$COI = \frac{525nm - 473nm}{525nm + 473nm} \tag{3}$$

The COI (3) exhibits a marginally higher ROC AUC (Area Under the Receiver Operating Characteristic Curve), a measure of classification accuracy, at 0.9855 compared to the NDVI's 0.9744. This improvement in performance, visible in Figure 4's histogram distributions of the COI, is characterized by a distinct tail for vegetation. Consequently, Figure 5a illustrates the COI's enhanced capability in accurately classifying healthier biological patches.

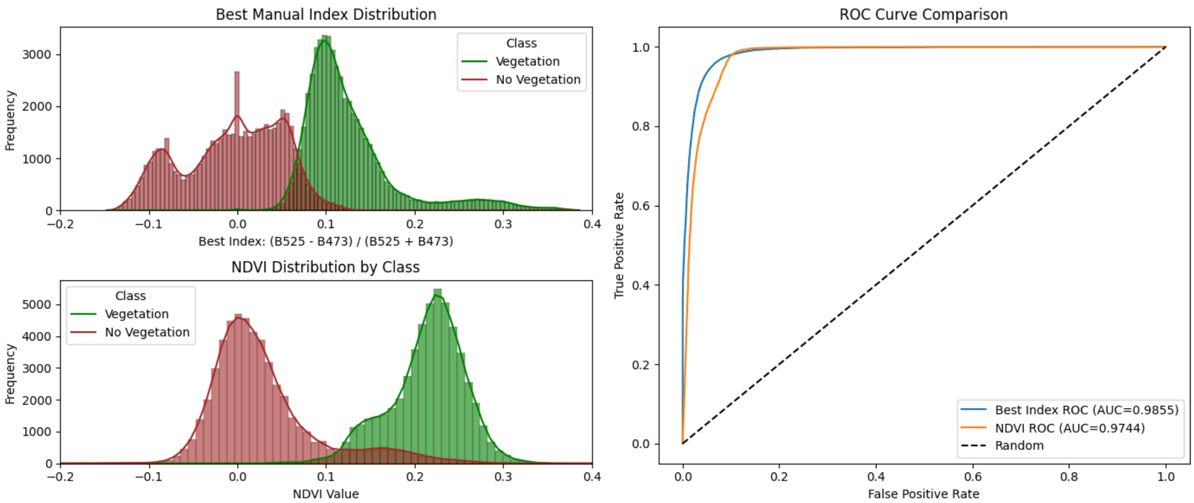

Figure 4: Histogram distributions and ROC curves comparing COI and NDVI classification capabilities.

Figure 5b integrates the COI's enhanced fidelity with the NDVI's robust overall discrimination by multiplying both indices. This combination yields an index that robustly handles varying wall angles and effectively distinguishes between vegetation health states.

XGBoost [12] classification is additionally employed on the annotated point cloud, utilizing all available bands. Figure 5c validates the method's effectiveness in identifying biological growth. XGBoost also facilitates analyzing feature importance for classification tasks. Figure 6 displays the ten most influential bands based on annotated training data, highlighting the significant role of RGB bands in differentiating vegetation from other building materials. Furthermore, applying XGBoost solely to RGB data demonstrates substantial potential for vegetation detection in this scenario, as presented in Figure 5d.

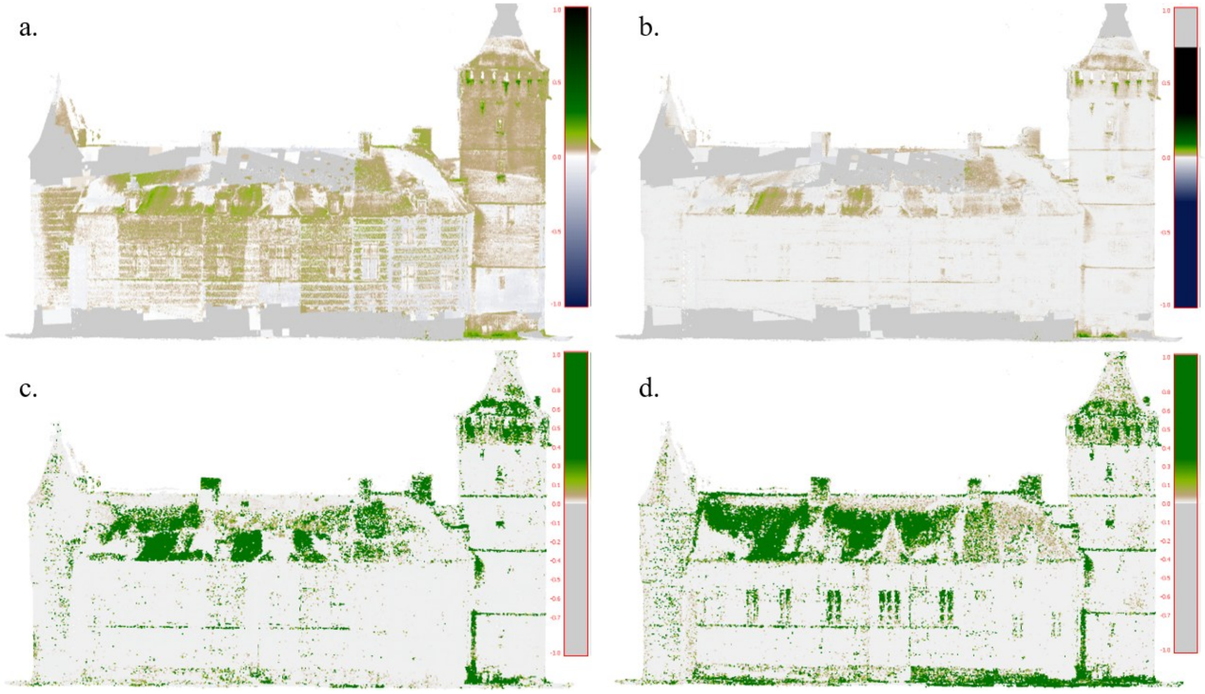

Figure 5: Classification comparisons:
a. COI; b. NDVI × COI; c. XGBoost (HSI and RGB); d. XGBoost (RGB only).

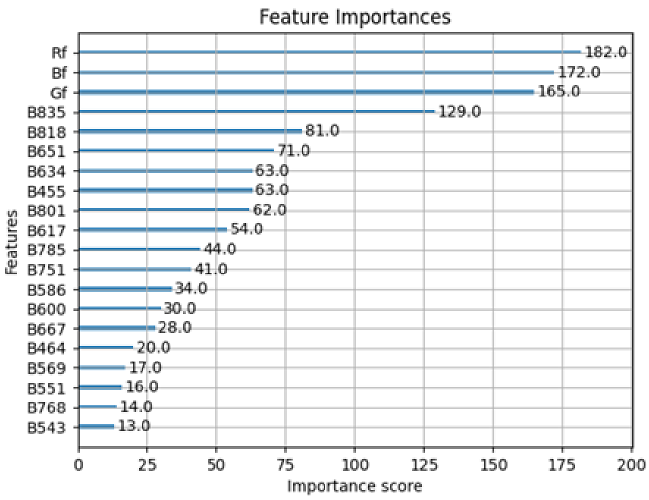

Figure 6: XGBoost features importance, from binary classification.

5. CONCLUSION

This study confirms that vegetation on cultural heritage façades can be accurately detected using non-invasive techniques such as hyperspectral and RGB imaging within the VIS–NIR range. The XGBoost classifier demonstrates that sufficient spectral information is available to distinguish biological growth from other façade materials, even in a complex architectural context such as the Castle of Horst.

The proposed Case Optimized Index (COI), derived through a brute-force spectral band search, achieves improved classification performance over the traditional NDVI. While NDVI remains a widely used and valuable index, its limitations, particularly under varying illumination conditions and non-standard viewing angles, reduce its reliability in heritage applications. Combining NDVI with the COI results in a more robust index, capable of capturing both general vegetation presence and finer distinctions in biological health.

These findings highlight that no single normalized difference index is universally sufficient. Instead, combining indices or complementing them with machine learning approaches, such as XGBoost, leads to significantly improved accuracy. Feature importance analysis further underlines the value of RGB bands, reinforcing their practical relevance when hyperspectral data is limited or unavailable. Future research is needed to validate the importance of RGB bands across diverse datasets and case studies.

To generalize the results of this research, future work should expand the dataset to include a broader range of vegetation types, health conditions, façade materials, and environmental factors. Including pollution as a third classification category may further enhance the accuracy and interpretability of façade condition assessments.

6. BIBLIOGRAPHY

[1] A. I. De Castro, Y. Shi, J. M. Maja, and J. M. Peña, 'UAVs for vegetation monitoring: overview and recent scientific contributions', *Remote Sensing*, vol. 13, no. 11, p. 2139, May 2021, doi: 10.3390/rs13112139.

[2] S. Huang, L. Tang, J. P. Hupy, Y. Wang, and G. Shao, 'A commentary review on the use of normalized difference vegetation index (NDVI) in the era of popular remote sensing', *J. For. Res.*, vol. 32, no. 1, pp. 1–6, Feb. 2021, doi: 10.1007/s11676-020-01155-1.

[3] F. J. Kriegler, 'Preprocessing transformations and their effects on multispectral recognition', in *Proceedings of the sixth international symposium on remote sensing of environment*, 1969, pp. 97–131.

[4] W. Rouse and R. H. Haas, 'Monitoring vegetation systems in the great plains with erts'.

[5] M. Hemmleb, F. Weritz, A. Schiemenz, A. Grote, and C. Maierhofer, 'Multi-spectral data acquisition and processing techniques for damage detection on building surfaces', presented at the Proceedings of the ISPRS Commission V Symposium 'Image Engineering and Vision Metrology', H. Maas and D. Schneider, Eds., Dresden, Germany: ISPRS, Sep. 2006, p. 6 pages.

[6] J. Valença, L. M. S. Gonçalves, and E. Júlio, 'Damage assessment on concrete surfaces using multi-spectral image analysis', *Construction and Building Materials*, vol. 40, pp. 971–981, Mar. 2013, doi: 10.1016/j.conbuildmat.2012.11.061.

[7] J. Sandino *et al.*, 'A Green Fingerprint of Antarctica: Drones, Hyperspectral Imaging, and Machine Learning for Moss and Lichen Classification', *Remote Sensing*, vol. 15, no. 24, Art. no. 24, Jan. 2023, doi: 10.3390/rs15245658.

[8] D. A. Chaghdo, B. Koirala, L. Cristina, R. Hayen, and P. Scheunders, 'Exploring the Potential of Hyperspectral Imaging to Estimate the Moisture Content in Natural and Historical Stones'.

[9] S. Del Pozo, J. Herrero-Pascual, B. Felipe-García, D. Hernández-López, P. Rodríguez-Gonzálvez, and D. González-Aguilera, 'Multispectral Radiometric Analysis of Façades to Detect Pathologies from Active and Passive Remote Sensing', *Remote Sensing*, vol. 8, no. 1, Art. no. 1, Jan. 2016, doi: 10.3390/rs8010080.

[10] B. Koirala and P. Scheunders, 'An efficient method for water content estimation of building materials from spectral reflectance', *NDT & E International*, vol. 147, p. 103214, Oct. 2024, doi: 10.1016/j.ndteint.2024.103214.

[11] P. Soubrier, R. Muszyński, M. Vlaminck, H. Luong, and N. Van Den Bossche, 'Automated Inspection of Heritage Sites: UAV RGB and Hyperspectral Photogrammetry Applied to Castle of Horst', in *2024 14th Workshop on Hyperspectral Imaging and Signal Processing: Evolution in Remote Sensing (WHISPERS)*, Helsinki, Finland: IEEE, Dec. 2024, pp. 1–5. doi: 10.1109/WHISPERS65427.2024.10876505.

[12] T. Chen and C. Guestrin, 'XGBoost: A Scalable Tree Boosting System', in *Proceedings of the 22nd ACM SIGKDD International Conference on Knowledge Discovery and Data Mining*, Aug. 2016, pp. 785–794. doi: 10.1145/2939672.2939785.